AIP Advances

Acoustic spin pumping in magnetoelectric bulk acoustic wave resonator

Cite as: AIP Advances **6**, 056306 (2016); https://doi.org/10.1063/1.4943765
Submitted: 06 November 2015 • Accepted: 30 December 2015 • Published Online: 08 March 2016

N. I. Polzikova, S. G. Alekseev, I. I. Pyataikin, et al.

View Online Export Citation CrossMark

ARTICLES YOU MAY BE INTERESTED IN

Spin wave generation by surface acoustic waves
Journal of Applied Physics **122**, 043904 (2017); https://doi.org/10.1063/1.4996102

Acoustic spin pumping: Direct generation of spin currents from sound waves in Pt/$Y_3Fe_5O_{12}$ hybrid structures
Journal of Applied Physics **111**, 053903 (2012); https://doi.org/10.1063/1.3688332

Magnons parametric pumping in bulk acoustic waves resonator
Applied Physics Letters **117**, 072408 (2020); https://doi.org/10.1063/5.0022267

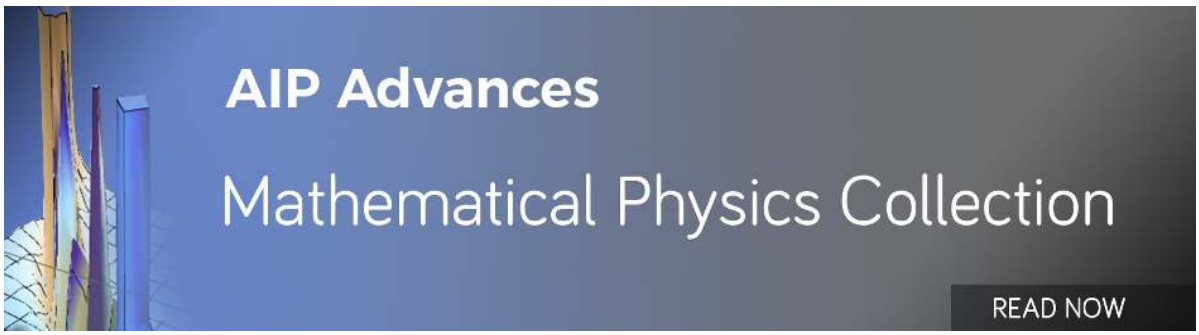

AIP Publishing

© 2016 Author(s).

Acoustic spin pumping in magnetoelectric bulk acoustic wave resonator

N. I. Polzikova,[a] S. G. Alekseev, I. I. Pyataikin, I. M. Kotelyanskii, V. A. Luzanov, and A. P. Orlov
Kotel'nikov Institute of Radio Engineering and Electronics of Russian Academy of Sciences, Mokhovaya 11, building 7, Moscow, 125009, Russia

(Presented 13 January 2016; received 6 November 2015; accepted 30 December 2015; published online 8 March 2016)

We present the generation and detection of spin currents by using magnetoelastic resonance excitation in a magnetoelectric composite high overtone bulk acoustic wave (BAW) resonator (HBAR) formed by a Al-ZnO-Al-GGG-YIG-Pt structure. Transversal BAW drives magnetization oscillations in YIG film at a given resonant magnetic field, and the resonant magneto-elastic coupling establishes the spin-current generation at the Pt/YIG interface. Due to the inverse spin Hall effect (ISHE) this BAW-driven spin current is converted to a dc voltage in the Pt layer. The dependence of the measured voltage both on magnetic field and frequency has a resonant character. The voltage is determined by the acoustic power in HBAR and changes its sign upon magnetic field reversal. We compare the experimentally observed amplitudes of the ISHE electrical field achieved by our method and other approaches to spin current generation that use surface acoustic waves and microwave resonators for ferromagnetic resonance excitation, with the theoretically expected values. © *2016 Author(s). All article content, except where otherwise noted, is licensed under a Creative Commons Attribution 3.0 Unported License.* [http://dx.doi.org/10.1063/1.4943765]

I. INTRODUCTION

A pure spin current is a flux of a spin angular momentum not accompanied by charge transfer and in contrast to a conventional current is totally non-dissipative.[1] The problem of finding an efficient pure spin current source for spintronic devices with lower power consumption is quite topical today.

Spin current generation methods widely applied at present are dynamical methods based on electromagnetic excitation of ferromagnetic resonance (FMR), magnetostatic or spin waves in hybrid paramagnetic metal/magnetic material structures.[2–4] It is clear that spin current generation based on these methods is most efficient in materials with low electric and magnetic losses. Ferrimagnetic materials of the rare-earth ferrite-garnet group, especially yttrium iron garnet (YIG), meet these criteria best.

In addition to the electrodynamic methods, the possibility for pure spin current generation (acoustic spin pumping (ASP)) based on acoustic driving magnetic dynamics both under magnetoelastic resonance (MER)[5–7] and the off-resonance conditions[8–10] has been demonstrated. Since the elastic energy can be nearly completely transformed into magnetic energy under MER, it seems that the resonance generation methods are much more efficient than off-resonances ones. It should be noted that spin current generation using the acoustic method is most efficient if materials with low propagation losses, such as YIG or gadolinium - gallium garnet (GGG), are used.

In pioneering work[5] surface acoustic waves (SAW) were used for magnetic dynamics resonance excitation. Since MER is generally excited in the gigahertz frequency range, the ninth harmonic of a low-frequency (172 MHz) interdigital transducer (IDT) was used. Using high harmonics

[a]Author to whom correspondence should be addressed. Electronic mail: polz@cplire.ru

 ©Author(s) 2016

causes significant loss of efficiency in transforming electromagnetic energy supplied to the IDT into acoustic energy.

In this paper, we propose ASP by using MER excitation in a magnetoelectric composite high overtone bulk acoustic wave (BAW) resonator (HBAR) formed by a Al-ZnO-Al-GGG-YIG-Pt structure. Magnetic dynamics in the YIG film is excited and detected by an electroacoustic transducer (Al-ZnO-Al). This resonator allows, firstly, relatively simple excitation of microwave (1-4 GHz) range BAW by using a piezoelectric transducer formed by traditional optical (not submicron) lithography operating at low transducer harmonics. Secondly, it can be used to store elastic energy efficiently and concentrate it strictly within a working space that is a cylinder with a base formed by the transducer aperture (with area approximately 0.03 mm^2) and a height equal to the resonator thickness. The use of such a small working volume allows to reduce the requirement for magnetic field uniformity, in principle making it possible to create chip sources of pure spin current, in which the bias magnetic field is formed by miniature strips of high coercivity rare earth-Fe-Co-B system magnets instead of bulky electric magnets. Combination of all these properties makes it possible to hope that the new method of ASP proposed will be quite efficient and competitive.

Previously in Refs. 11–15 we showed theoretically and observed experimentally that excitation of nonuniform FMR occurs in a Al-ZnO-Al-GGG-YIG HBAR at frequencies close to the ones of MER in the magnetic material (YIG). This effect manifests itself as HBAR resonance frequency shift in the vicinity of the MER.

In this study, we use the composite resonator described above as a pure spin current source: magnetic dynamics excited acoustically in the YIG film is used for spin current pumping into the layer of platinum deposited on YIG. To detect spin current, we use the method based on measuring the voltage caused by the inverse spin Hall effect (ISHE)[2] – the appearance of a potential difference at the edges of a film of material with high spin-orbit coupling (platinum in our case) caused by conversion of the spin current absorbed in it. This voltage depends directly on the spin current that allows comparing the efficiency of the ASP proposed both with traditional pumping methods employ microwave cavities[2,3] or strip lines[4] for FMR excitation and with the acoustic generation method exploits SAW.[5]

II. EXPERIMENT

A schematic of the composite BAW resonator is shown in Fig. 1(a). The resonator consists of a gadolinium-gallium garnet (GGG) plate with (111) orientation and 1 mm in thickness. A t_F = 50-micron film of Ga, Sc-substituted YIG with $Y_3(Fe_{2-y}Sc_y)(Fe_{3-x}Ga_x)O_{12}$, $y \approx 0.26$, $x \approx 1.03$ composition characterized by lower saturation magnetization $4\pi M_s \approx 350$ G[16] and low cubic anisotropy fields ($H_c \approx$ -3 .. -4 Oe)[17–19] was grown on one side of the plate by liquid-phase epitaxy. Such low values of these parameters allow magnetic dynamics excitation in this material at frequencies near 1 GHz, where HBARs usually have the greatest Q factor. Another advantage of Ga-substituted YIG is its high thermal stability (20 times as great as that for pure YIG).[20]

The Gilbert damping, α_G^{HBAR}, of the (Ga, Sc) - YIG film studied was estimated to be $5.1 \cdot 10^{-5}$.[21] This value is nearly 2.5 times greater than those reported for bulk pure YIG ($2 \cdot 10^{-5}$).

A piezoelectric transducer was deposited on the other side of the GGG plate. It consists of a 3 μm thick piezoelectric textured ZnO film sandwiched between two 150-200 nm thick Al electrodes. The top and the bottom electrodes were patterned by optical lithography as shown in Fig. 1(b). For primarily transverse BAW excitation, ZnO film was deposited by magnetron sputtering so that its texture axis **c** formed a 40°- 45° angle to the normal of the GGG plate.[22] Notice that in some frequency ranges such a transducer generates longitudinal BAWs as well (see Fig. 1(d)).

To detect the inverse spin Hall effect, a Pt stripe t_{Pt} = 12 nm thick, 300 μm width and with the sheet resistivity of $R_\square$ = 21 Ohm/□ was deposited by magnetron sputtering on the surface of the YIG film underneath the acoustic resonator. After that we reduced the width of the stripe to a width less than the diameter of the acoustic aperture, d, by focused-ion-beam milling (see Fig. 1(b)).

We used a S-parameter network analyzer connected to a calibrated microwave probe to excite the resonator. Fig. 1(c) shows its reflection spectrum $|S_{11}(f)|$ measured near the frequency

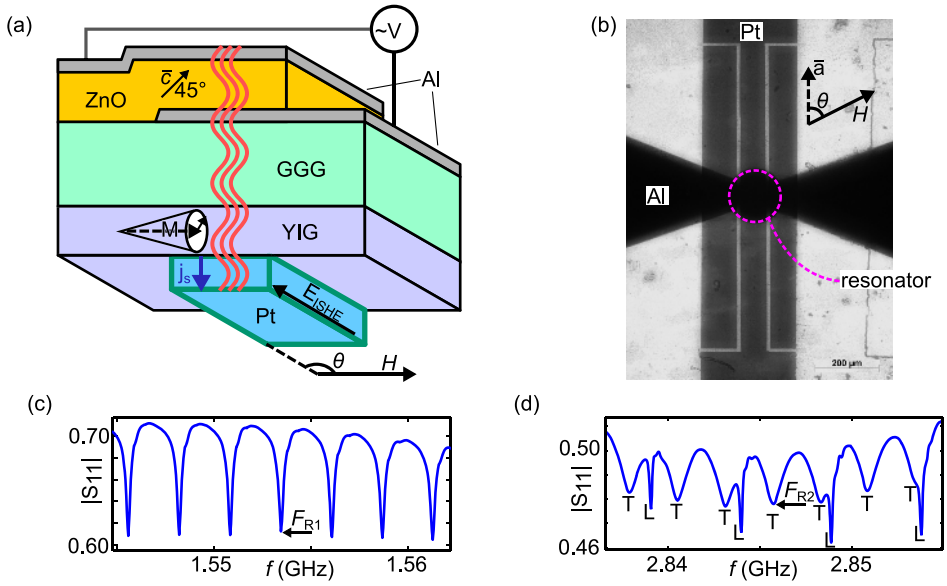

FIG. 1. (a) Schematic of Al-ZnO-Al-GGG-YIG-Pt HBAR for ASP. The rf voltage V is applied across the piezoelectric transducer formed by the ZnO film (***c*** - [0001] texture axis) sandwiched between thin-film aluminum electrodes. The transducer launches and detects a BAW, which propagates vertically. (b) Transmitted light micrograph of HBAR. The results of the structure micrograph superimposition with the focusing: on the lower plane with Pt stripe on it (grey region), and on the upper plane with the piezoelectric transducers on it (black region – the transducer electrodes). A circle with diameter d marks the overlap area of the top and the bottom electrodes (the active region of the resonator). (c), (d) $|S_{11}|$ as a function of frequency in the vicinity of MER at F_{R1} (c) and F_{R2} (d). The resonance peaks corresponding to longitudinal (L) and transversal (T) waves are marked in (d).

$F_{R1} = 1.55336$ GHz. The distance between adjacent dips on $|S_{11}|$ plot is 2.6 MHz, which corresponds to transverse wave resonances for this structure. The figure shows that longitudinal BAWs are not excited in this frequency range. A fragment of the spectrum in the vicinity of frequency $F_{R2} = 2.846$ GHz is shown for comparison in Fig. 1(d). As can be seen, longitudinal waves are excited together with transverse ones, and the efficiency of transverse waves excitation is much lower in this region than at F_{R1}. Further measurements were performed in an external static magnetic field $\boldsymbol{H}$ applied within the YIG film plane at an angle θ to the axis **a** of the Pt stripe (see Fig. 1(b)).

To determine the fields corresponding to MER at the selected resonance frequencies F_{R1} and F_{R2}, the evolution of the curve $|S_{11}(f)|$ shape in the magnetic field applied was studied. The resonance frequency shifts (±50 kHz) were observed at $H_{R1} \approx 400$ Oe and $H_{R2} \approx 800$ Oe in agreement with Kittel's equation $F_{R1,2} \cong \gamma\sqrt{H_{R1,2}(H_{R1,2} + 4\pi M_s)}$, where $\gamma \approx 2.8$ MHz/Oe. Such a behavior agrees with previously published data for HBAR with epitaxial films of pure YIG.[15]

After determining the region of magnetic fields corresponding to MER, the voltage on the platinum, $U(f, H)$, was detected by conventional lock-in technique with a 1.2207 kHz amplitude modulation of the rf signal exciting HBAR.

III. RESULTS AND DISCUSSION

The dependence of dc electric field E in the Pt strip versus magnetic field H (390 Oe $\leq H \leq$ 408 Oe) and frequency f (F_{R1} - 1 MHz $\leq f \leq F_{R1}$ + 1 MHz) is shown in Fig. 2(a).[23]

The dependence $E(f, H)$ both on frequency and magnetic field has a resonant character. The coordinates of position of the maximum are (F_{R1} – 26 kHz, 401.57 Oe). The cross-section of 3D surface depicted in Fig. 2(a) with the plane $H_{R1} = 401.57$ Oe is shown in Fig. 2(b), where the frequency dependence of the reflectivity $|S_{11}|$ in the vicinity of the resonance at F_{R1} is also given. As follows, the width (≈ 0.5 MHz) of the peaks and their position (near F_{R1}) are correlated closely with each other. It should be noted that the shape of the resonance curve $E(f, H_{R1})$, and the shift of

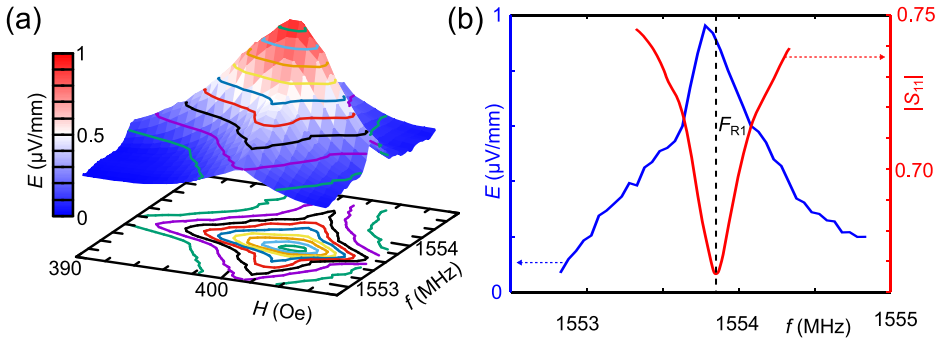

FIG. 2. Resonant character of electrical field E in Pt strip at $\theta = 90°$. (a) E as a function of frequency f and magnetic field H near (F_{R1}, H_{R1}). (b) Comparing the frequency dependences of $E(f, H_{R1})$ (blue) and the reflectivity modulus $|S_{11}|$ (red).

its maximum to the frequency slightly less than F_{R1} are in agreement with the results of simulation performed in Ref. 24.

The dependence of $E(f,H)$ similar to the one shown in Fig. 2(a) is also observed in the vicinity of the HBAR resonance at F_{R2} and magnetic field $H_{R2} \approx 800$ Oe. However in this case the value of E (F_{R2}) in resonance maximum is significantly less than $E(F_{R1})$. The value of the $|S_{11}|^2$ dip ($\Delta|S_{11}(F_{R2})|^2$) is also considerably reduced comparing with ($\Delta|S_{11}(F_{R1})|^2$), as can be seen from Fig. 1(c) and Fig. 1(d). This points out that the voltage on the Pt strip is determined by the acoustic power $\sim \Delta|S_{11}|^2 \cdot P_{rf}$,[5] where P_{rf} is the electromagnetic power supplied.

It should be noted that no electrical voltage U was sensibly detected out of the range of transversal BAW resonance and under HBAR excitation at frequencies corresponding longitudinal BAW. The whole set of mentioned facts allows us to claim that the voltage U and hence the field E are connected with MER in HBAR under study.

Let us consider how U depends on the relative orientation of stripe axis, **a,** and magnetic field $\boldsymbol{H}$ (see Fig 1(b)). The dependences of the detected voltage U versus magnetic field detuning $\delta H = H - H_{R1}$ are shown in Fig. 3 for several angles θ. As follows, the voltage reaches its maximal value when the field direction is perpendicular to the stripe and goes to zero when they are parallel. The voltage changes its sign upon magnetic field reversal.

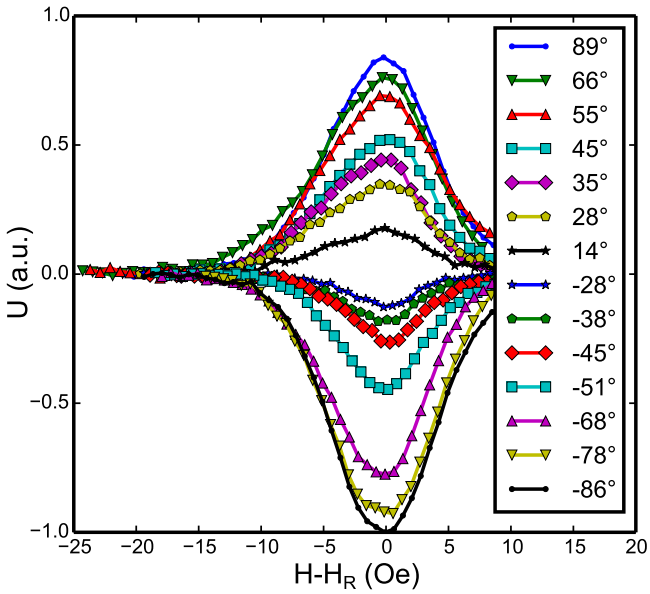

FIG. 3. Dependences of measured voltages U on the Pt stripe as a function of magnetic field detuning δH for various directions of $\boldsymbol{H}$. Reference for the angle θ is shown in Fig. 1(b). Resonance field $H_{R1} \approx 402$ Oe.

The whole data set obtained shows that the detected voltage U on the Pt stripe is induced by the electric field $E = E_{\mathrm{ISHE}} \sim [\boldsymbol{j}_s, \boldsymbol{M}_s] \sim \Delta|S_{11}|^2 P_{\mathrm{rf}} \sin\theta$, caused by the inverse spin Hall effect[2,3] ($\boldsymbol{j}_s$ is spin current density generated at YIG/Pt interface under MER excitation). This verifies that the HBAR on the basis of Al-ZnO-Al-GGG-YIG structure is a source of pure spin current.

Let us compare the field E_{ISHE} caused by the ASP proposed in this work and the analogous fields produced by the approaches to spin current generation that use SAW[5] and microwave resonators (MWR)[3] for FMR excitation. Since $E_{ISHE} \propto g_r h_{rf}^2/(\alpha_G^2 t_{Pt} f)$,[25] there is a need to determine the value of high frequency driving magnetic field h_{rf} exciting FMR (or spin waves) and spin mixing conductance $g_r \propto M_s t_{FM}(\alpha_G^{FM/NM} - \alpha_G^{FM})$.[25] The latter strongly depends on ferromagnet (FM)/normal metal (NM) interface quality that is characterized by the difference, $\alpha_G^{FM/NM} - \alpha_G^{FM} = \xi \alpha_G^{FM}$, where $\xi \geq 1$ corresponds to good FM/NM interface while $\xi << 1$ corresponds to poor interface.[26,27] In the case of ASP the driving magnetic field is an effective field $h_{rf} = h_{ME} = b_2 k_{MER} u$ of magnetoelastic origin.[28] The estimation of h_{ME} using the relation $h_{ME} = h_{ME}^{HBAR} \cong\cong b_2 k_{MER} \sqrt{8\Delta|S_{11}|^2 P_{rf}/\left[\pi d^2 \rho v_t (2\pi f)^2\right]}$ and parameters from Refs. 28 and 29 shows that at rather low power $P_{rf} = 5$ mW supplied to HBAR, $h_{ME}^{HBAR} \approx 0.5$ Oe. This field exceeds the one used for spin pumping with MWR in Ref. 3 ($h_{rf}^{MWR} \approx 0.11$ Oe, at $P_{rf} \approx 1$ mW) and is nearly equal to the field produced by SAW method[5] ($h_{ME}^{SAW} \approx 0.73$ Oe, at $P_{rf} \approx 1000$ mW). This is a certain advantage of our method.

Using the introduced notations, we obtain the following relations for the ratios of the fields generated by different methods (HBAR, MWR and SAW):

$$E_{ISHE}^{HBAR}/E_{ISHE}^{MWR} = \xi^{HBAR}/\xi^{MWR} \cdot M_s^{HBAR}/M_s^{MWR} \cdot \alpha_G^{MWR}/\alpha_G^{HBAR} \cdot t_{Pt}^{MWR}/t_{Pt}^{HBAR} \cdot f^{MWR}/f^{HBAR} \cdot (h_{ME}^{HBAR}/h_{rf}^{MWR})^2 \approx 30 \cdot \xi^{HBAR}/\xi^{MWR},$$

$$E_{ISHE}^{HBAR}/E_{ISHE}^{SAW} = \xi^{HBAR}/\xi^{SAW} \cdot M_s^{HBAR} t_F^{HBAR}/(M_s^{SAW} t_F^{SAW}) \cdot \alpha_G^{SAW}/\alpha_G^{HBAR} \cdot R_{sq}/(Rw/L) \cdot (h_{ME}^{HBAR}/h_{rf}^{SAW})^2 \approx 17 \cdot \xi^{HBAR}/\xi^{SAW},^{30} \quad (1)$$

where in the last expression we have taken into account that $f^{HBAR} \cong f^{SAW}$ and $R_{sq} = R_{\square}$. At the same time the experimental ratios, $E_{ISHE}^{HBAR}/E_{ISHE}^{MWR}$ and $E_{ISHE}^{HBAR}/E_{ISHE}^{MWR}$, are both about unity (see Ref. 31). That is an order of magnitude less than those which would be expected from Eq. (1) at comparable quality of the interfaces, namely, when $\xi^{HBAR} \cong \xi^{MWR}, \xi^{SAW}$.

In summary, for the first time the generation of pure spin current in HBAR based on Al-ZnO-Al-GGG-YIG-Pt hybrid under resonant excitation of the magnetic dynamics in YIG by BAW has been demonstrated. According to our estimates, at rather low power, $P_{rf} = 5$ mW, supplied to the HBAR, the high frequency magnetic field reaches significant amplitude of the order of 0.5 Oe. At the same time, improving the quality of YIG/Pt interface is mainly needed to further enhance the efficiency of the ASP proposed.

ACKNOWLEDGMENTS

This work was supported by grants 13-07-01006, 13-07-12416, and 16-07-01210 from the Russian Foundation for Basic Research. We are grateful to Alexey Temiryazev for providing us with GGG - (Ga, Sc)-YIG structures and helpful discussion.

[1] S. Maekawa, S. O. Valenzuela, E. Saitoh, and T. Kimura, *Spin Current* (Oxford University Press, Oxford, 2012), p. 179.
[2] E. Saitoh, M. Ueda, H. Miyajima, and G. Tatara, Applied Physics Letters **88**, 182509 (2006).
[3] Y. Kajiwara, K. Harii, S. Takahashi, J. Ohe, K. Uchida, M. Mizuguchi, H. Umezawa, H. Kawai, K. Ando, K. Takanashi, S. Maekawa, and E. Saitoh, Nature **464**, 262 (2010).
[4] O. Mosendz, J. E. Pearson, F. Y. Fradin, G. E. W. Bauer, S. D. Bader, and A. Hoffmann, Physical Review Letters **104**, 046601 (2010).
[5] M. Weiler, H. Huebl, F. S. Goerg, F. D. Czeschka, R. Gross, and S. T. B. Goennenwein, Physical Review Letters **108**, 176601 (2012).
[6] L. Dreher, M. Weiler, M. Pernpeintner, H. Huebl, R. Gross, M. S. Brandt, and S. T. B. Goennenwein, Physical Review B **86**, 134415 (2012).
[7] L. Thevenard, C. Gourdon, J. Y. Prieur, H. J. von Bardeleben, S. Vincent, L. Becerra, L. Largeau, and J. Y. Duquesne, Physical Review B **90**, 094401 (2014).

[8] K. Uchida, H. Adachi, T. An, T. Ota, M. Toda, B. Hillebrands, S. Maekawa, and E. Saitoh, Nature Materials **10**, 737 (2011).
[9] K. Uchida, T. An, Y. Kajiwara, M. Toda, and E. Saitoh, Applied Physics Letters **99**, 212501 (2011).
[10] K. Uchida, H. Adachi, T. An, H. Nakayama, M. Toda, B. Hillebrands, S. Maekawa, and E. Saitoh, Journal of Applied Physics **111**, 053903 (2012).
[11] N. I. Polzikova and G. D. Mansfeld, in *Proceedings of the 1998 IEEE Ultrasonic Symposium*, *Sendai, Japan*, *5-8 October 1998*, edited by S. C. Schneider, M. Levy, and B. R. MacAvoy (IEEE, Piscataway, NJ, 1998), pp. 967–970.
[12] N. I. Polzikova, A. O. Raevskii, and A. S. Goremykina, J. Commun. Technol. Electron. **58**, 87 (2013).
[13] N. Polzikova, S. Alekseev, I. Kotelyanskii, and A. Raevskiy, in *IEEE International Ultrasonics Symposium*, *Prague, Czech Republic*, *21-25 July 2013* (IEEE, Piscataway, NJ, 2013), pp. 216-219.
[14] N. Polzikova, S. Alekseev, I. Kotelyanskii, A. Raevskiy, and Y. Fetisov, Journal of Applied Physics **113**, 17C704 (2013).
[15] N. Polzikova, S. Alekseev, I. Kotelyanskii, and A. Raevskiy, in *IEEE International Frequency Control Symposium*, *Taipei, Taiwan*, *19-22 May 2014* (IEEE, Piscataway, NJ, 2014), pp. 127-130.
[16] G. T. Kazakov, A. V. Maryakhin, B. P. Nam, A. G. Sukharev, Y. A. Filimonov, I. V. Shein, Y. I. Surov, and R. Y. Margolina, Pis'ma v Zhurnal Tekhnicheskoi Fiziki **14**, 1733 (1988).
[17] S. L. Vysotskii, G. T. Kazakov, B. P. Nam, A. V. Maryakhin, A. G. Sukharev, Y. A. Filimonov, and A. S. He, Fizika Tverdogo Tela **34**, 1376 (1992) [Soviet Physics. Solid State **34**, 731 (1992)].
[18] S. L. Vysotsky, G. T. Kazakov, A. V. Maryakhin, B. P. Nam, A. G. Sukharev, Y. A. Filimonov, and A. S. He, Radiotekhnika i Elektronika **37**, 1086 (1992) [Soviet J. Commun. Technol. Electron. **37**, 92 (1992)].
[19] A. G. Temiryazev, M. P. Tikhomirova, P. E. Zil'berman, A. V. Maryakhin, and A. S. Khe, Pis'ma v Zhurnal Tekhnicheskoi Fiziki **19**, 75 (1993) [Technical Physics Letters **19**, 631 (1993)].
[20] H. Le Gall, J. P. Castera, P. Hartemann, and D. Mahasoro, IEEE Transactions on Magnetics **22**, 990 (1986).
[21] A least-square fit to the data-set #2 in Fig. 1 of Ref. 19 with function $\Delta H = \Delta H_0 + f4\pi\alpha_G/(\gamma\sqrt{3})$ yields $\alpha_G \approx 5.1\cdot10^{-5}$ and $\Delta H_0 \approx 0.19$ Oe, where the latter is the inhomogeneous broadening and γ is the gyromagnetic ratio.
[22] N. F. Foster, G. A. Coquin, G. A. Rozgonyi, and F. A. Vannatta, IEEE Transactions on Sonics and Ultrasonics **15**, 28 (1968).
[23] The field was calculated by using the relation $E = U/d$, where U is the measured voltage, $d = 0.168$ mm is the length of the Pt stripe segment located underneath the BAW transducer (see Fig. 1(b)).
[24] A. Kamra, H. Keshtgar, P. Yan, and G. E. W. Bauer, Physical Review B **91**, 104409 (2015).
[25] H. L. Wang, C. H. Du, Y. Pu, R. Adur, P. C. Hammel, and F.Y. Yang, Physical Review Letters **112**, 197201 (2014).
[26] Note that in YIG g_r scales linearly with t_F while $t_F < 200$ nm, and saturates at higher t_F (see for example Ref. 27).
[27] M. B. Jungfleisch, A. V. Chumak, A. Kehlberger, V. Lauer, D. H. Kim, M. C. Onbasli, C. A. Ross, M. Kläui, and B. Hillebrands, Physical Review B **91**, 134407 (2015).
[28] Here b_2 is the magnetoelastic coupling constant, $b_2 = B_2/M_s \approx 3\cdot10^4$ erg/(cm^3·G) for (Ga, Sc)-YIG (see Ref. 29); k_{MER} is the wave vector corresponding MER, $k_{MER} \approx 3\cdot10^4$ cm^{-1}; u is an elastic displacement; $\Delta|S_{11}|^2 \approx 0.132$ as follows from Fig. 1(c); $\rho \approx 5.17$ g/cm^3, $v_t \approx 3.9\cdot10^5$ cm/s, are YIG density and transversal velocity, respectively.
[29] Y. A. Filimonov, Doctoral Thesis, Moscow, 2008 (in Russian).
[30] We put here $t_F^{HBAR} = 200$ nm, see Ref. 26. $Rw/L = 37\ \Omega\cdot0.375$ mm/0.5 mm $\approx 27.8\ \Omega$, see Ref. 5.
[31] $E_{ISHE}^{HBAR} \approx 1$ μV/mm, see Fig. 2(b), $E_{ISHE}^{MWR} \approx 4$ μV/3 mm = 1.3 μV/mm, see Ref. 3, $E_{ISHE}^{SAW} \approx 0.8$ μV/0.5 mm = 1.6 μV/mm, see Ref. 5.